DALTON

Vibrational and solid-state phosphorus-31 nuclear magnetic resonance spectroscopic studies of 1:1 complexes of PPh_3 with gold(I) halides; crystal structure of [AuBr(PMe_3)]†

Klaus Angermair,[a] Graham A. Bowmaker,*[b] Eban N. de Silva,[b] Peter C. Healy,[c] Brian E. Jones[b] and Hubert Schmidbaur[a]

[a] *Anorganisch-Chemisches Institut der Technischen Universität München, D-85747 Garching, Germany*
[b] *Department of Chemistry, University of Auckland, Private Bag 92019, Auckland, New Zealand*
[c] *School of Science, Griffith University, Nathan, Queensland 4111, Australia*

The crystal structure of [AuBr(PMe_3)], like that of the corresponding chloride, was found to consist of three crystallographically independent molecules linked through weak Au • • • Au contacts to form helical chains. The Au • • • Au distances [3.648(1), 3.980(2), 3.548(2) Å] are, however, significantly longer than in the chloro- and iodo-complexes, implying that the Au • • • Au interaction is weakest in the bromide. The far-IR and Raman spectra of [AuX(PMe_3)] (X = Cl, Br or I) have been measured, and assignments made for the bands observed. The spectra were analysed to see whether they show any effects of the weak Au • • • Au bonding evident in the crystal structures. In particular, the low-wavenumber limit of previously reported Raman spectra for these species has been extended in order to search for $\nu(Au_2)$ bands. The X = Cl or I compounds show a strong Raman band which can be assigned to the δ(PAuX) deformation, but no $\nu(Au_2)$ bands were found in the region predicted on the basis of recent assignments for such modes in other complexes which display Au • • • Au contacts of similar length. Possible reasons, including an interaction between $\nu(Au_2)$ and δ(PAuX) modes, are discussed. The solid-state cross polarization magic angle spinning ^{31}P NMR spectra of the chloride and iodide complexes consist of doublets due to the presence of $^1J(^{197}Au–^{31}P)$ coupling. This is a rare observation of spin–spin coupling between the spin $I = \frac{1}{2}$ ^{31}P nucleus and the strongly quadrupole coupled ^{197}Au nucleus, and permits estimation of the $^1J(^{197}Au–^{31}P)$ coupling constants for these complexes.

Complexes of gold(I) with phosphine ligands have been known for many years,[1–3] but there has been a recent resurgence of interest in compounds of this type since many show unexpected interactions between the closed-shell d^{10} metal centres.[4–16] These Au • • • Au interactions are believed to be due to relativistic effects.[17–19] In a recent study of one such complex, $[Au_2(dmpm)_2][PF_6]_2$ [dmpm = bis(dimethylphosphino)-methane], a strong Raman band at 68 cm^{-1} was assigned to $\nu(Au_2)$, the vibration of the Au_2 unit which has an Au • • • Au separation of 3.045(1) Å. Comparison of this with data for a number of other entities containing Au_2 units resulted in a correlation between the force constant for the $\nu(Au_2)$ vibration and $r(Au_2)$, the distance between the two Au atoms. The correlation encompassed $r(Au_2)$ values in the range 2.4–3.6 Å.[20] All of the complexes which were involved in this study were ones in which the two gold centres are linked by bridging ligands. There are a number of complexes in which the Au • • • Au interaction occurs between separate molecules.[4–11] The simplest examples involve the 1:1 adducts of gold(I) halides with trimethylphosphine, which have structures in which the individual [AuX(PMe_3)] molecules are linked *via* Au • • • Au interactions to form dimers (X = I) or chain polymers (X = Cl) with $r(Au_2)$ contacts of 3.168 (X = I),[4] 3.271, 3.356 and 3.386 Å (X = Cl).[5] In the present study we report the structure of the X = Br complex, which forms a helical chain polymer similar to that of the chloride, with $r(Au_2)$ = 3.548, 3.648 and 3.980 Å. The infrared and Raman spectra of [AuX(PMe_3)] were reported some time ago,[21] but the Raman spectra were not measured in the region below 100 cm^{-1} where, on the basis of the correlation mentioned above, the $\nu(Au_2)$ vibrations would be expected to occur. We have therefore re-examined the vibrational spectra of these complexes, and have extended the Raman measurements further into the lower-wavenumber region in order to investigate the possible existence of $\nu(Au_2)$ bands there.

The [AuX(PMe_3)] complexes are also of interest in connection with the solid-state NMR behaviour of complexes involving a spin $I = \frac{1}{2}$ nucleus coupled to a spin $I > \frac{1}{2}$ nucleus.[22–27] We have previously shown that the cross-polarization magic angle spinning (CP MAS) ^{31}P NMR spectra of [AuX(PPh_3)] and $[HgX(PPh_3)]^+$ show doublets due to spin–spin coupling to the $I = \frac{3}{2}$ ^{197}Au and ^{201}Hg nuclei, coupling which is not normally observed due to the rapid spin–lattice relaxation which is associated with these strongly quadrupole coupled metal nuclei.[28,29] However, such splitting was not observed in the case of [AuX(tmpp)] [tmpp = tris(2,4,6-trimethoxyphenyl)phosphine],[30] suggesting that the nature of the phosphine ligand is a factor in the observation of such coupling. We have therefore recorded the CP MAS ^{31}P NMR spectra of [AuX(PMe_3)] in order to investigate this question further.

Experimental

Preparations

Trimethylphosphine was prepared by a literature method.[31] Chloroauric acid $HAuCl_4$ (Univar) was used without further purification. Bromo(dimethyl sulfide)gold(I), [AuBr(SMe_2)], was prepared by a literature method.[32] Chloro(trimethylphosphine)gold(I), [AuCl(PMe_3)], was prepared from chloroauric acid and PMe_3 by a modification of the literature method reported previously for the corresponding PEt_3 complex.[33] M.p. 219–222 °C (lit.,[21] 230–231 °C). Its identity was confirmed by the infrared spectrum.[21] Tetra-*n*-butylammonium diiodo-

† *Non-SI unit-employed:* dyn = 10^{-5} N.

aurate(I), $[NBu_4][AuI_2]$, was prepared by a previously described method.[30] Tetra-*n*-butylammonium dibromoaurate(I), $[NBu_4][AuBr_2]$, was synthesized by reduction of $[NBu_4][AuBr_4]$ with acetone according to a previously described method.[34]

Bromo(trimethylphosphine)gold(I), [AuBr(PMe$_3$)]. This was prepared by two different methods.

(*a*) Trimethylphosphine (0.11 g, 1.42 mmol) was slowly added, dropwise, to a suspension of $[AuBr(SMe_2)]$ (0.49 g, 1.42 mmol) in tetrahydrofuran (thf) (30 cm^3). The solvent and the liberated SMe_2 were removed under vacuum and the raw product was vacuum dried. The complex $[AuBr(PMe_3)]$ was obtained as a colourless crystalline solid from dichloromethane solution by slow addition of diethyl ether.

(*b*) In a 25 cm^3 Schlenk tube $[NBu_4][AuBr_2]$ (2.05 g, 3.42 mmol) was dissolved in warm dimethylformamide (dmf) (3.5 cm^3). The solution was degassed and placed under a nitrogen atmosphere. To this was added PMe_3 (0.26 cm^3, 1.93 mmol) slowly, with stirring, whereupon the solution became hot. After standing for approximately 5 min the solution yielded a white solid and this was filtered off and washed with the minimum volume of chilled dimethylformamide before being vacuum dried. The crude product was recrystallized from dmf (2.5 cm^3). Yield 0.32 g (36% based on Au). M.p. 224–227 °C (lit., 232–233 °C).[21]

Iodo(trimethylphosphine)gold(I), [AuI(PMe$_3$)]. In a 25 cm^3 Schlenk tube $[NBu_4][AuI_2]$ (2.0 g, 2.89 mmol) was dissolved in dimethylformamide (3.5 cm^3). The solution was degassed and placed under a nitrogen atmosphere. To this was added PMe_3 (0.3 cm^3, 2.89 mmol) dropwise, with shaking. Initially, as the PMe_3 was added, the solution went black, but as more was added the solution became clear and heat was evolved. After standing for a short period it yielded a white solid which was filtered off, washed with the minimum of chilled dimethylformamide and vacuum dried. Yield 0.99 g (86%). The IR and Raman spectra of the product were identical to those previously reported.[21]

X-Ray crystallography

Crystals of $[AuBr(PMe_3)]$ were obtained by slow evaporation of the solvent from a chloroform solution. A suitable single crystal was transferred at solid CO_2 temperature under an argon atmosphere into a glass capillary and the capillary was sealed.

Crystal data. C_3H_9AuBrP, M_r = 352.95, colourless crystals of dimensions 0.03 × 0.11 × 0.35 mm, triclinic, space group $P\bar{1}$ (no. 2), a = 9.841(1), b = 9.923(1), c = 13.003(1) Å, α = 74.48(1), β = 75.31(1), γ = 71.34(1)°, Z = 6, U = 1137.6 Å^3, D_c = 3.087 g cm^{-3}, $F(000)$ = 936.

Enraf-Nonius CAD4 diffractometer, Mo-Kα radiation (λ = 0.710 69 Å), T = +23 °C. Data were corrected for Lorentz-polarization effects and for absorption [μ(Mo-Kα) = 247.7 cm^{-1}]. The structure was solved by direct methods and refined by full-matrix least-squares calculations against F (SHELXTL PLUS).[35] From 5272 measured reflections, 2844 were considered 'observed' [$F_o > 4\sigma(F_o)$] and used for refinement. All hydrogen atoms were calculated in idealized geometry and allowed to ride on their corresponding C atoms with isotropic contributions [$U_{iso(fix)}$ = 0.08 Å^2]. The non-H atoms were refined with anisotropic displacement parameters. The structure converged for 164 refined parameters to an R (R') value of 0.0574 (0.0677). The function minimized was $[\Sigma w(|F_o| - |F_c|)^2/\Sigma w F_o^2]^{\frac{1}{2}}$, where $w = 1/[\sigma^2(F_o) + 0.001\,195\,(F_o)^2]$. Residual electron densities: +1.72, −2.92 e Å^{-3} (located at Au and Br).

Atomic coordinates, thermal parameters and bond lengths and angles have been deposited at the Cambridge Crystallographic Data Centre (CCDC). See Instructions for Authors, *J. Chem. Soc., Dalton Trans.*, 1996, Issue 1. Any request to the CCDC for this material should quote the full literature citation and the reference number 186/124.

Spectroscopy

Infrared spectra were recorded at 4 cm^{-1} resolution at room temperature as KBr discs on a Digilab FTS-60 Fourier-transform spectrometer employing an uncooled DTGS detector. Far-infrared spectra were recorded at 2 cm^{-1} resolution at room temperature as pressed Polythene discs on a Digilab FTS-60 Fourier-transform spectrometer employing an FTS-60V vacuum optical bench with a 6.25 μm mylar film beam splitter (75–500 cm^{-1}) or a 12.5 μm beam splitter (40–250 cm^{-1}), a mercury lamp source and a pyroelectric triglycine sulfate detector. Raman spectra were recorded at 4.5 cm^{-1} resolution using a Jobin-Yvon U1000 spectrometer equipped with a cooled photomultiplier (RCA C31034A) detector. The 488.0 nm exciting line from a Spectra-Physics model 2016 argon-ion laser was used. Solid-state CP MAS ^{31}P-{^{1}H} NMR spectra were obtained at ambient temperature on a Varian Unity-400 spectrometer at 161.92 MHz. Single contact times of 2 ms were used with a proton pulse width of 6.5 μs, a proton decoupling field of 60 kHz and a recycle delay time of 45 s. The samples were packed in Kel-F inserts within silicon nitride rotors and spun at a speed of 5 kHz at the magic angle. A total of 32 free induction decays were collected and transformed with an experimental line broadening of 10 Hz. Chemical shift data are referenced to 85% H_3PO_4 *via* an external sample of solid PPh_3 (δ −9.9).

Results and Discussion

Syntheses

The complex $[AuCl(PMe_3)]$ was readily synthesized from chloroauric acid and PMe_3 by the literature method which was originally reported for the corresponding PEt_3 complex.[33] This original study reported a method for the preparation of $[AuI(PEt_3)]$ which involves preliminary reaction of chloroauric acid with iodide.[33] This latter reaction has subsequently been shown to yield gold(I) iodide, AuI.[36] However, reaction of $HAuCl_4$ with KI in a 1:6 mole ratio, followed by addition of PMe_3, yielded a dark brown mixed product which was shown by far-IR spectroscopy to contain $[Au(PMe_3)_2]^+$ [$\nu_{sym}(PC_3)$ 349 cm^{-1}], as well as the desired $[AuI(PMe_3)]$ complex [$\nu_{sym}(PC_3)$ 370, ν(AuI) 164 cm^{-1}]. The far-IR spectrum also showed a number of bands (141, 125, 95 cm^{-1}) which may be due to polyiodide species [*e.g.* ν_{asym}(I–I) 140 cm^{-1} for I_3^-].[37] Another previously published route for the preparation of $[AuI(PMe_3)]$ using halide exchange between $[AuCl(PMe_3)]$ and potassium iodide[21] also proved to be unsatisfactory, as it was difficult to exchange all of the chloride without severely reducing the yield of pure product. We therefore used a modification of a previous method involving displacement of iodide from $[AuI_2]^-$.[30] The bromide complex was prepared in a similar manner by displacement of Br^- from $[AuBr_2]^-$, as well as by displacement of SMe_2 from $[AuBr(SMe_2)]$ by PMe_3.

Crystal structure of [AuBr(PMe$_3$)]

The crystal structure of $[AuBr(PMe_3)]$ is shown in Fig. 1, and selected distances and angles are compared in Table 1 with those for the corresponding chloride and iodide complexes. The molecular arrangement is nearly identical to that found in the previously studied chloride[5] and cyanide[38] compounds. However, in contrast to these two compounds, which form polymeric chain structures with Au • • • Au distances of about

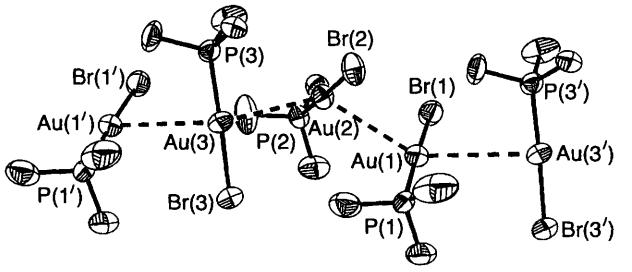

Fig. 1 Part of the crystal lattice of [AuBr(PMe_3)], showing the formation of a helical chain through the presence of weak Au · · · Au interactions

Table 1 Selected distances (Å) and angles (°) for [AuX(PMe_3)] complexes

Parameter	X = Cl[a]	Br[b]	I[c]
Au(1)–X(1)	2.310(4)	2.419(3)	2.583(1)
Au(2)–X(2)	2.306(4)	2.415(3)	
Au(3)–X(3)	2.310(1)	2.415(3)	
Au(1)–P(1)	2.234(4)	2.242(7)	2.256(3)
Au(2)–P(2)	2.233(3)	2.235(5)	
Au(3)–P(3)	2.234(3)	2.228(6)	
Au(1) · · · Au(2)	3.356(1)	3.648(1)	3.168(1)
Au(2) · · · Au(3)	3.271(1)	3.548(2)	
Au(1) · · · Au(3')	3.386(1)	3.980(2)	
P(1)–Au(1)–X(1)	179.4(1)	177.1(2)	178.46(6)
P(2)–Au(2)–X(2)	177.5(2)	176.5(2)	
P(3)–Au(3)–X(3)	178.4(2)	177.9(2)	
Au(1)–Au(2)–Au(3)	141.8(1)	133.9(1)	
Au(1)–Au(3)–Au(2)	141.9(1)	133.8(1)	
Au(2)–Au(1)–Au(3')	141.6(1)	133.4(1)	

[a] Ref. 5; the atom numbering has been altered to correspond to that in Fig. 1. [b] This work. [c] Ref. 4.

3.3 Å, the intermolecular Au · · · Au distances in the bromide are significantly longer, with Au(1) · · · Au(2), Au(2) · · · Au(3) and Au(1) · · · Au(3') of 3.648(1), 3.548(2), 3.980(2) Å respectively (Table 1). This suggests the presence of a weak Au · · · Au interaction, at least in the case of the first two of the above, so that the structure can be considered as being made up of trimers involving the Au(1) · · · Au(2) · · · Au(3) contacts with separations of about 3.6 Å. The geometries of the three inequivalent monomeric [AuBr(PMe_3)] molecules show no unusual features. The Au–P distances are equal (within experimental error) to those of the corresponding chloro complex, but are significantly shorter than that in the iodo complex, where the molecules aggregate as dimers rather than as infinite chains.[4]

The Au · · · Au distances for [{AuX(PH_3)}$_2$] dimers have been calculated by MP-2 theory, yielding the values 3.366, 3.338 and 3.315 Å for X = Cl, Br and I respectively.[19] The corresponding distances in the crystal structures of [AuX(PMe_3)] are 3.34, 3.60 and 3.168 Å [average values for X = Cl or Br, excluding the long Au(1) · · · Au(3') distance in the bromide as discussed above]. The most remarkable difference between the the trends in the theoretical and the observed values occurs for the X = Br case, where the observed Au · · · Au is much greater than that calculated and the observed and calculated values for the chloride and iodide. Inclusion of the long Au(1) · · · Au(3') distance in the average for the bromide increases this discrepancy still further. Naturally the situation is complicated by the fact that [AuX(PMe_3)] display different degrees of aggregation in the solid state: dimers for X = I, chain polymers for X = Cl or Br. However, the chloride and bromide possess isomorphous crystal lattices, and it might have been expected that these would show a decrease in the average Au · · · Au from X = Cl to Br according to the theoretical predictions mentioned above. However, it is known that the Au · · · Au interaction is quite weak, not much stronger than other intermolecular forces.[12–14] The observed Au · · · Au distances in the solids are therefore likely to be strongly influenced by other non-bonded interactions, and so can probably not be considered as indicative of the inherent strength of the Au · · · Au interaction on its own.

Vibrational spectra

The far-IR and low-frequency Raman spectra of [AuX(PMe_3)] are shown in Figs. 2 and 3 and the wavenumbers and assignments of the low-frequency bands are given in Table 2. The spectra in the region above 500 cm^{-1} contain only bands due to the co-ordinated PMe_3, and these did not change much in position or relative intensity from one complex to another. The spectra were similar to that previously reported for [$Ag_4I_4(PMe_3)_4$].[39] The assignment of the lower-wavenumber spectra was made with reference to the assignments in this latter work, together with those in earlier studies of the present compounds.[21,40]

The ν(AuX) assignments are the same as those made previously for X = Cl or I; a strong band at 312 cm^{-1} with a shoulder at 305 cm^{-1} due to the $^{35,37}Cl$ isotopic splitting is replaced by a band at 164 cm^{-1} in going from the chloride to the iodide, and these wavenumbers are similar to those observed previously for other [AuX(L)] complexes (Table 3).[28,41–43] The X = Br case is unusual in that a strong doublet appears in the region 200–230 cm^{-1}, where ν(AuBr) is expected to occur, and examination of the spectra under higher resolution reveals that each component of the doublet is itself split into a doublet. The major splitting into two bands at about 200 and 230 cm^{-1} has been explained previously as being due to a mixing of ν(AuBr) with other internal coordinates such as ν(AuP), such that the two bands each have an approximately 50% contribution from ν(AuBr) in their potential-energy distributions.[40] The minor splitting is probably a space-group or factor-group effect; an alternative possibility is that it is due to an isotope effect arising from the presence of ^{79}Br and ^{81}Br, but it seems to be slightly too large for this. Further support for the assignment of these bands as predominantly ν(AuBr) comes from the fact that their average wavenumber is 214 cm^{-1}, exactly the same as ν(AuBr) in [AuBr(PEt_3)],[44] which fits in well with the observation that ν(AuCl) in [AuCl(PMe_3)] (312 cm^{-1}, Table 3) is almost identical to that of [AuCl(PEt_3)] (314 cm^{-1}).[44]

Comparison of the ν(MX) wavenumbers for [AuX(PMe_3)] with those for [AuX(PPh_3)] and [HgX(PPh_3)]$^+$ (Table 3) shows that there is a reduction in ν(MX) from the PPh_3 to the corresponding PMe_3 complex, and that this difference increases progressively along the series X = Cl, Br or I. This suggests that the Au–I bond in [AuI(PMe_3)] is relatively weak, and it can be noted that the Au–P bond in this complex is significantly longer than those in the other two halide compounds (Table 1). Both of these observations could possibly be related to the fact that this complex is the only one which forms a dimer, and that the Au · · · Au distance in the dimer is shorter than the mean Au · · · Au distances in the corresponding chloro- or bromo-complexes (Table 1). In this connection, it is of interest that in the recently reported [AuX(tmpp)] complexes, which involve a ligand which is strongly basic but much larger than PMe_3, the above trends are reversed, so that the Au–P and Au–I bonds appear to be relatively strong in comparison with corresponding chloro- and bromo-complexes.[30]

The assignment of the ν(AuP) mode has been the subject of considerable discussion in previous studies, and the band at about 380 cm^{-1} was assigned to this mode,[21,40] but it has been shown that considerable mixing takes place between the ν(AuP) and δ(PC_3) coordinates, and that a band at *ca.* 200 cm^{-1} also has some ν(AuP) character.[40] The problems associated with the assignment of ν(MP) modes in transition-metal complexes have

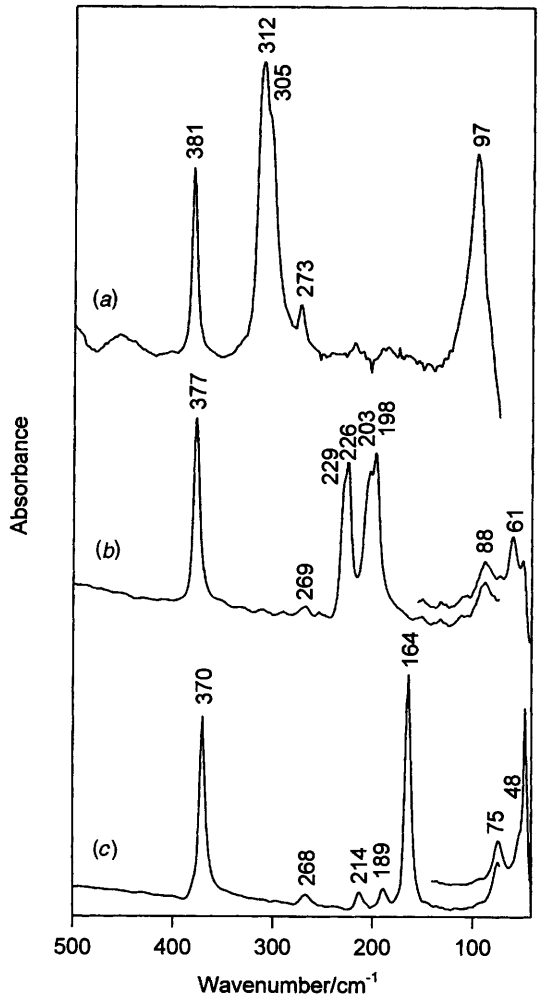

Fig. 2 Far-IR spectra of (*a*) [AuCl(PMe$_3$)], (*b*) [AuBr(PMe$_3$)] and (*c*) [AuI(PMe$_3$)]

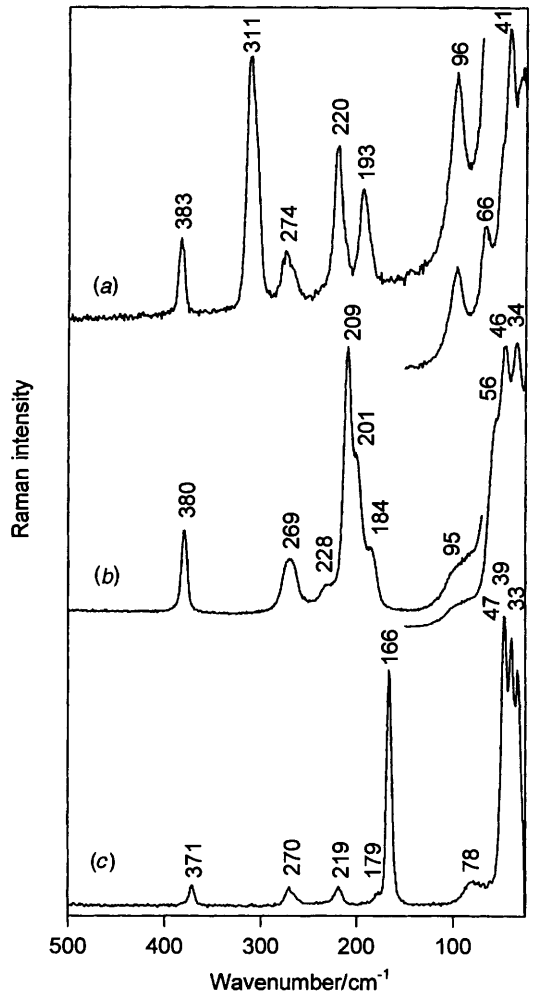

Fig. 3 Low-wavenumber Raman spectra of (*a*) [AuCl(PMe$_3$)], (*b*) [AuBr(PMe$_3$)] and (*c*) [AuI(PMe$_3$)]

Table 2 Wavenumbers (cm^{-1}) and assignments of the low-frequency bands in the IR and Raman spectra

[AuCl(PMe$_3$)]		[AuBr(PMe$_3$)]		[AuI(PMe$_3$)]		
IR	Raman	IR	Raman	IR	Raman	Assignment
381	383	377	379	370	371	$\delta_{sym}(PC_3)$ + ν(AuP)
273	274	269	269	268	270	$\delta_{asym}(PC_3)$
312	311	229	228	164	166	ν(AuX)
		226				
219	220	203	209	214	219	ν(AuP) + $\delta_{sym}(PC_3)$*
		198	201			
189	193		184	189	179	$\rho(PC_3)$
97	96	88	95	75	78	δ(PAuX)
		61		48	47	
	66		56		39	Lattice
	41		46		33	
	29		34			

* Includes a strong contribution from ν(MX) in the case X = Br (see text).

Table 3 Wavenumbers (cm^{-1}) assigned to ν(MP) and ν(MX) in [AuX(PMe$_3$)] and related species

	X = Cl		X = Br		X = I		
Compound	ν(MP)	ν(MX)	ν(MP)	ν(MX)	ν(MP)	ν(MX)	Ref.
[AuX(PMe$_3$)]	220	312	214[a]	214[a]	219	164	*b*
[AuX(PPh$_3$)]	182	329	173	234	159	189	41, 42
[AuX(PPh$_3$)$_2$]	164	221	160	139	158	119	42, 43
[HgX(PPh$_3$)]NO$_3$	164	321	161	231	147	188	28

[a] Average of multiple ν(AuBr) and ν(AuP) band positions (see text). [b] This work.

been discussed previously.[45] Bands have been assigned over a wide wavenumber range, 90–460 cm^{-1}, but definitive assignments have been made only in a few cases. Detailed studies involving metal isotope substitution have shown that ν(MP) modes occur at wavenumbers in the lower part of the above range, and that previous assignments in the range 360–380 cm^{-1} were too high.[46,47] For the Group 11 metals the most definitive assignments have been made for gold(I) complexes $[AuX(PPh_3)]$ and $[AuX(PPh_3)_2]$, yielding ν(AuP) values in the range 160–180 cm^{-1}.[41,42] The assignments of ν(MP) and ν(MX) for these and for $[HgX(PPh_3)]^+$ are compared with those assigned at *ca.* 200 cm^{-1} in the present work for $[AuX(PMe_3)]$ in Table 3. The ν(AuP) values for $[AuX(PMe_3)]$ are about 40–60 cm^{-1} higher than those for the corresponding PPh_3 complexes. However, the shift is in the expected direction for a change from the 'heavier' PPh_3 to the 'lighter' PMe_3 ligand. This type of dependence of ν(MP) on the nature of the phosphine ligand has been demonstrated previously.[46,47]

It is clear that the ν(AuP) assignments at *ca.* 200 cm^{-1} made for $[AuX(PMe_3)]$ in this work fit well with the other ν(MP) assignments in Table 3. However, as was pointed out in previous vibrational studies of these complexes, the distinction between ν(AuP) and the symmetric $\delta(PC_3)$ bending mode is rather artificial, as both vibrations have the same symmetry (A_1 under the idealized C_{3v} symmetry of the isolated molecules), so that some mixing of these coordinates will occur.[21,40] We have assigned the band at about 380 cm^{-1} to the symmetric $\delta(PC_3)$ bending mode, and the band at about 270 cm^{-1} to the asymmetric $\delta(PC_3)$ bending mode. These assignments are in line with those made for a number of complexes of PMe_3 with copper(I) or silver(I) halides.[39,48] The symmetry of the asymmetric $\delta(PC_3)$ mode (E under C_{3v}) is different from that of ν(AuP), so no mixing of these coordinates will occur in this case. The asymmetric $\delta(PC_3)$ frequency should thus be uninfluenced by changes in the Au–P bonding, unless such changes cause a change in the $\delta(PC_3)$ angle-bending force constant. In agreement with this, it is found that the frequency of this mode is essentially unchanged with change in halide in $[AuX(PMe_3)]$ (Table 2). In contrast, the frequency of the symmetric $\delta(PC_3)$ mode shows a significant halide dependence, the wavenumber of this band showing a slight decrease from the chloride to the iodide. This change can be attributed to coupling between the symmetric $\delta(PC_3)$ and the ν(AuP) coordinates.

In order to investigate the coupling of the ν(AuP) and $\delta(PC_3)$ modes in greater detail, we have carried out a partial normal coordinate calculation on $[AuI(PMe_3)]$. The calculation involved only the Au–I and Au–P bond stretching coordinates, and three PC_3 angle-bending coordinates. A combined atomic mass of 15.04 was used for the CH_3 groups, and the force constants used were as follows: k(Au–I) = 1.25, r^2k(CPC) = 0.2 mdyn $Å^{-1}$ (r = P–C bond length), k(Au–I, Au–P) = 0.2 mdyn $Å^{-1}$. The k(Au–I, Au–P) interaction constant used is similar to the k(Au–X, Au–X) constants determined previously for $[AuX_2]^-$.[34,49] The force constants k(Au–P), k(Au–I, Au–P) were varied from 0 to 1.0 and 0 to 0.2 mdyn $Å^{-1}$, respectively, in order to investigate the dependence of the wavenumbers of the various modes concerned on the strength of the Au–P interaction, and the results are shown in Fig. 4. Also included in Fig. 4 are the wavenumbers of diatomic Au–P and of diatomic Au–(PMe_3), in which the PMe_3 molecule is treated as a single atom of mass 76.08. As expected, $\delta_{asym}(PC_3)$, which has E symmetry under C_{3v}, does not mix with any of the other modes, which have A_1 symmetry, so the frequency of this mode is completely independent of k(Au–P). More surprising is the fact that ν(AuI) is essentially independent of k(Au–P), remaining constant at the value 166 cm^{-1} which is the vibrational frequency of a diatomic AuI unit with the k(Au–I) value given above. This provides some justification for the procedure which we have used in the past to calculate M–X force constants in $[(MXL_n)_m]$ complexes by considering the

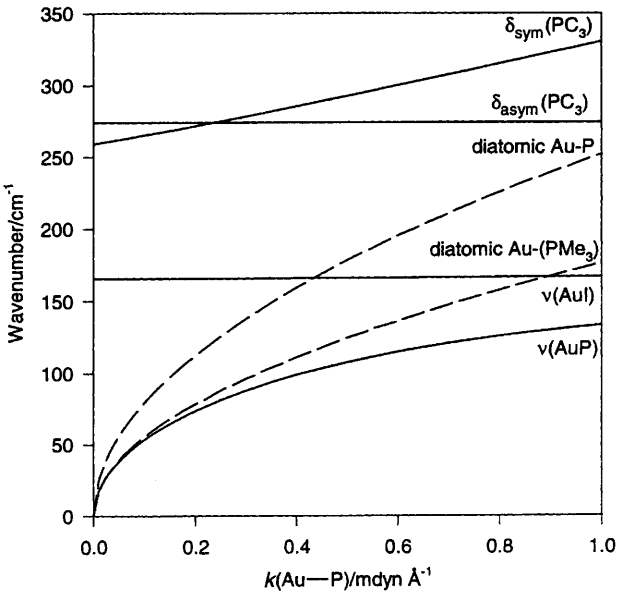

Fig. 4 Dependence of the wavenumbers of the ν(AuP), ν(AuI) and $\delta(PC_3)$ modes of an $[AuI(PMe_3)]$ monomer of C_{3v} symmetry on the k(Au–P) force constant (see text for details of the calculations)

$(MX)_m$ unit separately from the associated ligands L.[50,51] Both ν(AuP) and $\delta_{sym}(PC_3)$ increase with increasing k(Au–P) as a consequence of the coupling of these modes, both of which have A_1 symmetry. At low k(Au–P) values the extent of this mixing is small, and the description as ν(AuP) and $\delta_{sym}(PC_3)$ is a good approximation. As k(Au–P) increases, however, the degree of mixing changes, and on the basis of the potential-energy distribution *both* modes become predominantly ν(AuP) in character. As discussed above, previous studies involving metal isotope substitution have shown that ν(MP) modes occur in the 200 cm^{-1} region, and not above 300 cm^{-1} as had previously been suggested.[46,47] It is clear from the present calculations, however, that there is a significant component of ν(AuP) in $\delta_{sym}(PC_3)$, and this results in the ν(AuP) mode having a lower frequency than expected. This is evident in Fig. 4, which shows that ν(AuP) is always considerably lower than the frequency calculated for diatomic Au–P with the same force constant. More importantly, it is also significantly lower than the frequency calculated for 'diatomic' Au–(PMe_3), in which the PMe_3 is treated as a single atom with the mass of the whole PMe_3 molecule. As a consequence of this, ν(AuP) is lower than expected for the strength of the Au–P bond concerned. However, if $\delta_{sym}(PC_3)$ is assigned as ν(AuP) the reverse is true, as this frequency is considerably higher even than that for diatomic Au–P with the same force constant. The ν(AuP) values listed in Table 3 all lie within a fairly narrow range, and the results in Fig. 4 suggest a reason for this. For the higher values of k(Au–P), which correspond to the values in the complexes, ν(AuP) becomes relatively insensitive to changes in k(Au–P). It follows that complexes with significantly different values of this parameter will yield ν(AuP) values which do not differ as much from each other as would otherwise be expected. In concluding the discussion of Fig. 4 and its consequences one further point needs to be made. While the agreement between the calculated and experimental wavenumbers for ν(AuI) and $\delta_{asym}(PC_3)$ for all values of k(Au–P) is very good, the values ν(AuP) and $\delta_{sym}(PC_3)$ are too low. In the latter case the reason for this is that the calculated value of this frequency for k(Au–P) = 0 (which corresponds to an uncomplexed PMe_3 molecule) is too low by 45 cm^{-1} [for free PMe_3 $\delta_{asym}(PC_3)$ 263, $\delta_{sym}(PC_3)$ 305 cm^{-1}].[52] This could be corrected by carrying out a more complete normal coordinate analysis including the extra internal coordinates associated with the methyl groups. We have not done this here, since it was not our intention in this

study to obtain an exact force field for the complexes concerned. The aim was rather to assign the low-wavenumber bands and to indicate the factors which determine their positions in the spectra, and the partial analysis described above is sufficient for this.

Bands due to the $\rho(PC_3)$ rocking mode are assigned in the range 180–190 cm^{-1}, in agreement with an earlier study.[40] The present assignments can be compared with $\rho(PC_3)$ 220, ν(AuP) 156 cm^{-1} for $[Ag_4I_4(PMe_3)_4]$.[39,48] The reversal of the order of ν(MP) and $\rho(PC_3)$ in $[AuX(PMe_3)]$ seems reasonable, as the Au–P bond is expected to be considerably stronger than the Ag–P bond. As in the case of the asymmetric $\delta(PC_3)$ mode discussed above, the symmetry of the $\rho(PC_3)$ mode (E under C_{3v}) is different from that of ν(AuP) and ν(AuX), so its frequency should be fairly constant across the three halides, as is observed experimentally (Table 2).

The assignments of the δ(PAuX) bands in the far-IR spectra are similar to those reported previously,[21] but some differences have been noted, as discussed below. In the present study the lower wavenumber limit of the Raman spectra has been extended to about 25 cm^{-1}, and the Raman bands due to the δ(PAuX) modes for these complexes have also been observed (Table 2). For the bromide complex there are two bands in the IR spectrum at 61 and 88 cm^{-1} which are assigned to δ(PAuBr). The average wavenumber of these two bands is 75 cm^{-1}, almost identical to the assignment δ(PAuBr) 74 cm^{-1} made in the previous study. The iodide similarly shows two δ(PAuI) bands in the IR at 75 and 48 cm^{-1}, with an average of 62 cm^{-1}. The average values of the δ(PAuX) doublets (75, 62 cm^{-1} for X = Br or I respectively) agree well with the δ(XAuX) values for the corresponding $[AuX_2]^-$ ions (77, 63 cm^{-1}).[34] In the previously reported study of $[AuI(PMe_3)]$ only a single δ(PAuI) 47 cm^{-1} was reported.[21] Since the δ(PAuX) mode is doubly degenerate (E under local C_{3v} symmetry) a splitting is not unexpected. Possible reasons for this will be considered below.

In addressing the question of the possible existence of $\nu(Au_2)$ bands due to stretching of the Au · · · Au bonds the simplest case to consider is that of the $[AuI(PMe_3)]$ dimer, since the gold atoms are bonded in pairs in this case. According to the previously published linear correlation between the bond length $r(Au_2)$ and the logarithm of the force constant $k(Au_2)$,[20] the Au · · · Au distance of 3.168 Å observed in this complex (Table 1) corresponds to a force constant $k = 0.19$ mdyn $Å^{-1}$, which yields a predicted $\nu(Au_2)$ wavenumber of 57 cm^{-1}. This is in the middle of the range 36–71 cm^{-1} of $\nu(Au_2)$ wavenumbers for a number of Au · · · Au bonded species which were used to obtain this correlation.[20] In each case the $\nu(Au_2)$ band was measured from the Raman spectrum, where it occurred as the most intense low-wavenumber band. However, inspection of the Raman spectrum of $[AuI(PMe_3)]$ shows no band at the predicted wavenumber of 57 cm^{-1}. The only bands observed in this region have already been assigned to the δ(PAuI) vibrations of the monomer at 75, 48 cm^{-1} (IR) and 78, 47 cm^{-1} (Raman). This mode (E symmetry under C_{3v}) is predicted to be active in both the IR and Raman spectra, and the observed bands obey this selection rule. The $\nu(Au_2)$ mode is expected to be Raman active only (see below). The remaining unassigned bands in the Raman spectrum are those at 33 and 39 cm^{-1}. These lie well within the frequency range expected for lattice modes and while such modes could involve a contribution from Au · · · Au stretching they are well below the value 57 cm^{-1} which is predicted by the previously proposed correlation. The situation for $[AuCl(PMe_3)]$ is complicated by the more complex structure of this compound in the solid state, but it can be noted that comments similar to those made above about the Raman spectrum of the iodide also apply in this case. Thus, there is a Raman band at 96 cm^{-1} which coincides to the δ(PAuCl) band in the far-IR spectrum, and three bands at 29, 41 and 66 cm^{-1} in the lower-wavenumber region. The Au · · · Au distances in this complex (Table 1) yield predicted $\nu(Au_2)$ wavenumbers of 47 and 40 cm^{-1}. The fact that the Au atoms occur in chains in this complex rather than in pairs would affect these values to some extent (resulting in an increase in wavenumber by a factor between 1 and $\sqrt{2}$), so these wavenumbers lie in the region 40–70 cm^{-1}, where strong Raman bands occur (Fig. 3). It is therefore tempting to assign these bands to $\nu(Au_2)$. However, this does not fit in well with the negative result discussed above for the more strongly Au · · · Au bonded iodide, and further considerations in connection with the δ(PAuX) modes which are discussed below indicate that this is also not an acceptable assignment for the chloride.

The $\nu(Au_2)$ modes cannot be considered independently of the δ(PAuX) modes, since the wavenumbers proposed for the former are very similar to the known values of the latter, and displacement along the Au · · · Au coordinate will inevitably involve bending of the P–Au–X unit. For an idealized dimer of C_{2h} symmetry the displacement diagrams, symmetries, and activities of the modes involving these coordinates are shown in Fig. 5. The mode of B_u symmetry is IR active, and does not involve any Au · · · Au stretching. Thus the wavenumber of the δ(PAuX) mode in the IR spectrum gives the frequency of the pure bending mode. However, the two coordinates of A_g symmetry will mix if the frequencies of the appropriate motion are comparable. In order to determine the extent of this mixing we have carried out normal coordinate calculations on $(P–Au–X)_2$ dimers of C_{2h} symmetry. These calculations involved only the Au–P, Au–X and Au · · · Au bond-stretching coordinates, and the P–Au–X angle bending coordinates. A combined atomic mass of 76.07 was used for the PMe_3 molecule. The angle-bending force constants which reproduce the observed δ(PAuX) wavenumbers for the X = Cl or I complexes (the lower of the two wavenumbers in the case of the X = I complex) in isolated triatomic P–Au–X units were calculated as $(r_1r_2)^{\frac{1}{2}}k$(P–Au–X) = 0.087, 0.031 mdyn $Å^{-1}$ for X = Cl or I respectively (r_1, r_2 are the Au–P and Au–X bond lengths). These values were used as constants in the dimer calculations, and the Au · · · Au bond-stretching force constant $k(Au_2)$ was varied from 0 to 0.5 mdyn $Å^{-1}$. The results of these calculations for the $\nu(Au_2)$ and δ(PAuX) modes are shown in Fig. 6. The ν(AuP) and ν(AuX) frequencies were completely independent of $k(Au_2)$ and are omitted for clarity. Also shown are the frequencies of an isolated diatomic Au_2 unit. The results show that as $k(Au_2)$ increases the frequencies of the A_g $\nu(Au_2)$ and δ(PAuX) modes both increase. Thus the Raman band assigned to the δ(PAuX) mode should have a significantly higher wavenumber than that of the corresponding B_u IR band, which is completely independent of $k(Au_2)$. The experimental

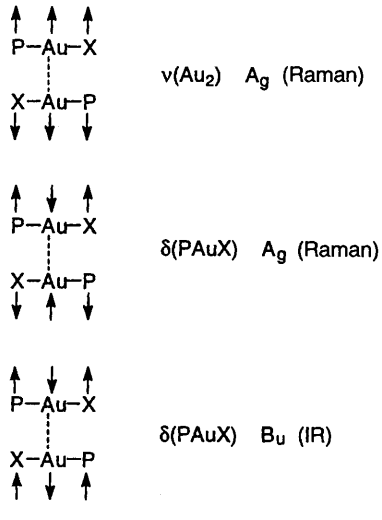

Fig. 5 Displacement diagrams, symmetries and activities of the modes involving $\nu(Au_2)$ and δ(PAuX) for an idealized dimer of C_{2h} symmetry

results show, however, that the Raman δ(PAuX) wavenumbers are almost identical (within experimental error) to the corresponding IR wavenumbers (Table 2). This suggests that the $\nu(Au_2)$ wavenumbers are very low indeed, perhaps lying below the lower accessible wavenumber limit of the spectra.

The results for the iodide dimer in Fig. 6 show that the concept of a '$\nu(Au_2)$' mode in such complexes is not as straightforward as has previously been assumed. In this case the extent of mixing of the A_g $\nu(Au_2)$ and δ(PAuI) modes is such that $\nu(Au_2)$ changes to δ(PAuI) [becoming independent of $k(Au_2)$ at higher values of this parameter] and the A_g δ(PAuI) mode changes to $\nu(Au_2)$ [its frequency asymptotically approaching that of the corresponding isolated diatomic Au_2 unit with increasing $k(Au_2)$]. At intermediate values of $k(Au_2)$ there are two modes with predominant $\nu(Au_2)$ character. The situation is completely analogous to that discussed above for the ν(AuP) mode, where mixing with $\delta_{sym}(PC_3)$ results in two modes with ν(AuP) character for certain values of k(Au–P). In the case of the iodide dimer, for which the Au · · · Au distance results in an estimated $k(Au_2) = 0.19$ mdyn Å^{-1}, the present calculations yield wavenumbers of 28 and 68 cm^{-1} for the two modes with $\nu(Au_2)$ character [the A_g $\nu(Au_2)$ and δ(PAuI) modes in Fig. 6]. The band nearest to this in the Raman spectrum is the weak one at 78 cm^{-1}. If this is the $\nu(Au_2)$ band it certainly does not stand out above the other bands in the same compound as the bands assigned as $\nu(Au_2)$ in the previous study of Au · · · Au bonded gold(I) complexes.[20] In fact the Raman band at 78 cm^{-1} lies close in wavenumber to the IR band at 75 cm^{-1}, and has been assigned to the higher-frequency component of the split δ(PAuI) mode, as discussed above.

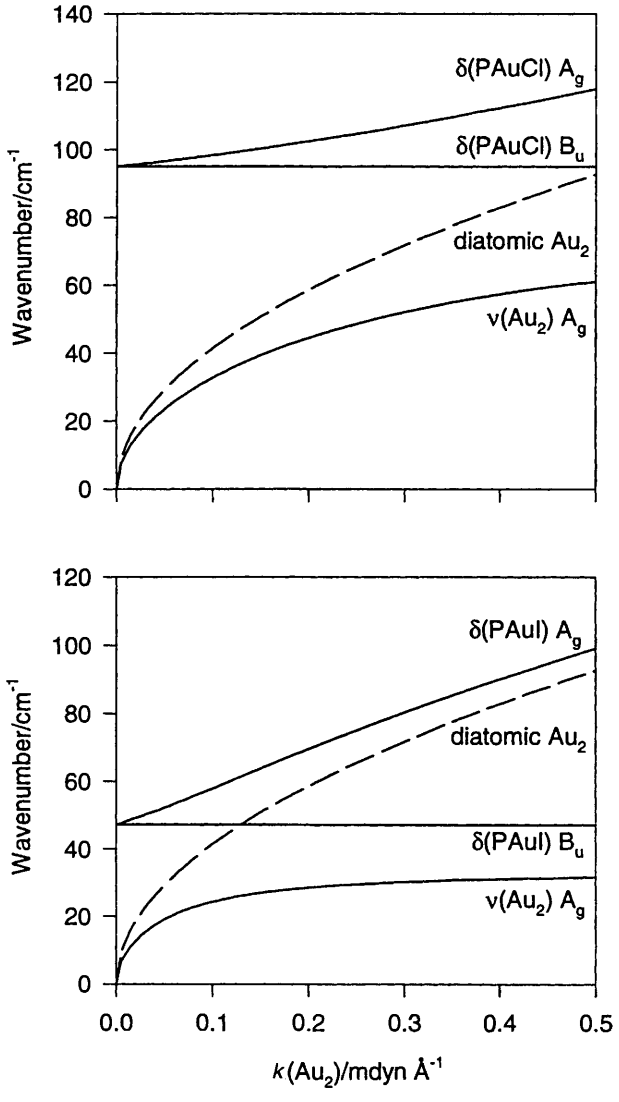

Fig. 6 Dependence of the wavenumbers of the $\nu(Au_2)$ and δ(PAuX) modes of a $(P–Au–X)_2$ dimer of C_{2h} symmetry on the $k(Au_2)$ force constant. Upper panel, X = Cl; lower panel, X = I (see text for details of the calculations)

These results raise questions about the previous assignments of $\nu(Au_2)$ modes. The data used in the previously published $r(Au_2)$ *vs.* ln $k(Au_2)$ correlation can be divided into two groups. One involves species containing formally singly bonded Au_2 with $r(Au_2) < 2.6$ Å, while the other involves formally non-bonded Au_2 with $r(Au_2) > 2.9$ Å.[20] The data for the former category are in little doubt as most of them are diatomic Au_2 species. The data for the latter species were obtained for compounds which are all more complex in structure than the PMe_3 compounds studied here, and their vibrational spectra were not interpreted in detail. The main criteria for the assignment of the $\nu(Au_2)$ bands were their high intensity in the Raman spectra, and the fact that the bands had the polarization behaviour predicted for the $\nu(Au_2)$ mode.[20] However, further support for these assignments has come from calculations on the Au · · · Au bonded dimeric species $[\{AuX(PH_3)\}_2]$.[19] A plot of $r(Au_2)$ *vs.* ln $k(Au_2)$ for these species is shown in Fig. 7. The best-fit line (1) is very close to

$$r(Au_2) = -0.248 \ln k(Au_2) + 2.79 \quad (1)$$

that determined previously for a different set of compounds.[20] One possible reason for the absence of a Raman band at the wavenumber predicted for the $[AuI(PMe_3)]$ dimer from these correlations is that the calculation of the wavenumber from the force constant uses a diatomic approximation, and the present work shows that this approximation is not valid when this wavenumber is comparable in magnitude to that of the internal P–Au–X bending mode. However, whatever the reason for this discrepancy, its existence casts some doubt on the utility of these correlations for the assignment of $\nu(Au_2)$ vibrations in the types of complex studied here. It is perhaps significant that the present study represents the first attempt to detect $\nu(Au_2)$ vibrations in compounds in which the Au · · · Au interaction occurs in the absence of ligands which act as a bridge between the two gold centres, but the reason for the absence of the strong $\nu(Au_2)$ Raman band which is predicted on the basis of the earlier studies on bridged systems remains uncertain.

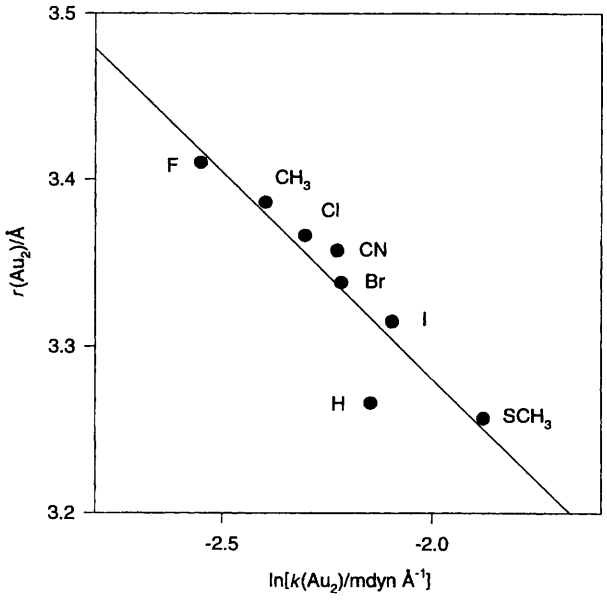

Fig. 7 Plot of $r(Au_2)$ *vs.* ln $k(Au_2)$ for $[\{AuX(PH_3)\}_2]$ (data from ref. 19)

Table 4 The CP MAS ^{31}P NMR chemical shifts δ and coupling constants J^*/Hz for [AuX(PMe_3)] and related species

	X = Cl		X = Br		X = I		
Compound	δ	^1J(MP)	δ	^1J(MP)	δ	^1J(MP)	Ref.
[AuX(PMe_3)]	−9.6	648	−6.9	—	−4.4	553	This work
[AuX(PPh_3)]	30.3	521	33.4	503	37.1	412	29
[HgX(PPh_3)]NO_3	30.5	3091	32.2	2727	33.0	2364	28

* $^1J(^{197}Au–P)$ or $^1J(^{201}Hg–P)$, all ± 100 Hz.

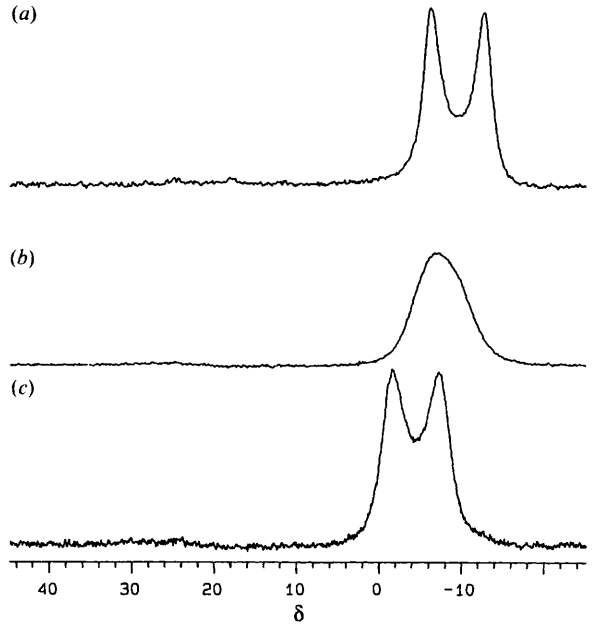

Fig. 8 The CP MAS ^{31}P NMR spectra of (*a*) [AuCl(PMe_3)], (*b*) [AuBr(PMe_3)] and (*c*) [AuI(PMe_3)]

CP MAS ^{31}P NMR Spectra

The solid-state CP MAS ^{31}P NMR spectra of [AuX(PMe_3)] are shown in Fig. 8, and the parameters obtained from the spectra are listed in Table 4. The spectra of the chloride and iodide compounds consist of doublets, which are considerably more clearly resolved than those of the corresponding PPh_3 complexes.[29] The doublet peak separations depend on X, being 1070 and 913 Hz (± 100 Hz) for X = Cl or I respectively. The large nuclear quadrupole moment of ^{197}Au (100% natural abundance, nuclear spin $I = \frac{3}{2}$) and the asymmetric co-ordination environment in these complexes would be expected to give rise to rapid quadrupolar relaxation, so that any $^1J(^{197}Au–^{31}P)$ scalar coupling would be averaged to zero, and the signal would appear as a narrow singlet.

The MAS NMR spectra of spin $I = \frac{1}{2}$ nuclei coupled to a quadrupolar nucleus have been discussed by various authors.[22–27] Menger and Veeman[22] reported calculations of the line positions in terms of the various coupling constants involved. For the case where the spin $I = \frac{1}{2}$ nucleus is ^{31}P and the quadrupolar nucleus is a metal atom M, the relevant coupling constants are the metal nuclear Zeeman interaction $Z = \gamma_M hB/2\pi$ (where γ_M is the magnetogyric ratio of the M nucleus), the metal nuclear quadrupole coupling constant $\chi = e^2qQ/h$ (e = electronic charge, q = electric field gradient at the M nucleus, Q = quadrupole moment of the M nucleus), the phosphorus–metal dipolar coupling constant D [equation (2),

$$D = (\mu_0/4\pi)(\gamma_P \gamma_M/r^3)(h/4\pi^2) \quad (2)$$

r = M–P bond length, μ_0 = vacuum permeability, γ_P = magnetogyric ratio of the ^{31}P nucleus] and the indirect spin–spin coupling constant J. The form of the spectrum depends on the ratio $R = D/J$ of the dipolar to the indirect coupling constant and on the dimensionless parameter K [equation (3),

$$K = -3\chi/4I(2I - 1)Z \quad (3)$$

I = spin of the M nucleus] which is proportional to the ratio of the copper quadrupole coupling constant to the copper nuclear Zeeman term. Menger and Veeman[22] have presented an analysis for three cases involving a metal nucleus M with spin $I = \frac{3}{2}$, where the spin $\frac{1}{2}$–spin $\frac{3}{2}$ interaction is purely dipolar, where it is purely scalar, and where mixed dipolar–scalar interactions exist. The most extensively studied case involves CP MAS ^{31}P NMR spectra of compounds containing Cu–P bonds, where asymmetric quartets are normally observed due to coupling of ^{31}P to the quadrupolar $^{63,65}Cu$ nuclei ($I = \frac{3}{2}$). In this case R lies in the range 0.5–1.0 and K lies in the range 0–0.5 and the observed spectra correspond to the case shown in Fig. 6 of Menger and Veeman.[22,53] As discussed previously in the analysis of the results for [AuX(PPh_3)] and [HgX(PPh_3)]$^+$,[28] R is much smaller than for the $^{63,65}Cu/^{31}P$ case, and the situation corresponds more closely to the case shown in Fig. 5 of Menger and Veeman.[22] The predicted four-line spectrum corresponding to $K \approx 0$ has been observed for the compounds [Au(dppen)$_2$]X[dppen = *cis*-1,2-bis(diphenylphosphino)ethylene; X = NO_3 or PF_6] in which near-tetrahedral co-ordination geometry about the Au atom is assumed to result in a ^{197}Au quadrupole coupling constant close to zero.[54] For complexes involving linear two-co-ordinate Au, however, the quadrupole coupling constant is expected to be much larger. The ^{197}Au quadrupole coupling constant in [AuCl(PPh_3)] is χ = 940 MHz,[55] and the gold-197 Zeeman interaction at 9.40 T is Z = 6.85 MHz, so that $K \approx 34$ [equation (3)]. It has been shown that for $K > 10$ the spectrum should consist of two lines with a spacing of about 1.65 times the $^1J(^{197}Au–^{31}P)$ coupling constant.[22,28] The values of the $^1J(^{197}Au–^{31}P)$ coupling constants calculated from the observed spacings of the doublets are listed in Table 4.

The decrease in $^1J(^{197}Au–^{31}P)$ from X = Cl to I follows a well established trend in ^1J(MP) values for metal halide complexes,[56] and can be attributed to a decrease in the 6s-electron density at the gold nucleus with decreasing positive charge on the gold atom. The factor by which the coupling constant is reduced is greater in [AuX(PMe_3)] than in [AuX(PPh_3)], but is similar to that in [HgX(PPh_3)]$^+$. The coupling constants for [AuX(PMe_3)] are greater than those for the corresponding [AuX(PPh_3)], perhaps reflecting the greater σ-donor strength of PMe_3 relative to PPh_3. They are also considerably greater than the value observed for [Au(dppen)$_2$]$^+$ (*ca.* 200 Hz),[54] and this follows the well established trend of a decrease in ^1J(MP) with an increase in the number of phosphine ligands bound to the metal atom M.[56]

These comparisons suggest that the $^1J(^{197}Au–^{31}P)$ values which result from the above analysis are of reasonable magnitude. They should, however, be regarded as very approximate at this stage. Further work is required to investigate the effects on the spectra of changes in the experimental conditions under which they are obtained, and to

explain why the effect is only observed in linear or nearly linear complexes with certain combinations of ligands.

The lack of splitting in the spectrum of the bromide complex in the present study is a feature which was not encountered in the previous studies of $[AuX(PPh_3)]$ or $[HgX(PPh_3)]^+$.[28,29] This presumably relates to some difference in the structure or dynamics of $[AuBr(PMe_3)]$ relative to the chloro- or iodo-analogues. The splitting of the CP MAS ^{31}P NMR signal is determined by the $^1J(^{197}Au–^{31}P)$ coupling constant, and the structural parameter which relates most directly to this is the Au–P bond length. The bromide complex shows a significantly greater degree of variation in this parameter than do the chloro- or iodo-complexes. Thus, the range of $^1J(^{197}Au–^{31}P)$ values for the bromide may be significantly greater than that for the other two complexes, resulting in a broadening and a consequent loss of resolution of the NMR signal. Alternatively, the lack of splitting may be due to a difference in the dynamics of the complex which affects aspects of the relaxation behaviour which determine whether the $^1J(^{197}Au–^{31}P)$ coupling effects are observable or not. In the absence of a suitable model for this process, nothing more can be said about this at present. However, our results provide further clear evidence that the appearance of this unusual coupling phenomenon is dependent on relatively subtle aspects of structure or dynamics, and should provide a good basis for testing theories concerning the origin of this effect. Despite the lack of splitting in the signal for the bromide complex, the ^{31}P chemical shift seems to behave in a normal fashion; the shifts for $[AuX(PMe_3)]$ show a regular upward progression from X = Cl to I in a similar manner to those for the other complexes in Table 4.

Acknowledgements

We acknowledge support of this work by grants from the New Zealand University Grants Committee, the University of Auckland Research Committee and the Australian Research Council. We thank Dr. Al Neilson for providing the trimethylphosphine which was used in this study, Mr. R. Buckley for the synthesis of $[NBu_4][AuBr_2]$, Ms. P. Harvey for recording the solid-state ^{31}P NMR spectra and Ms. A. Schier and Mr. J. Riede for handling the X-ray data set.

References

1 R. J. Puddephatt, *Comprehensive Coordination Chemistry*, ed. G. Wilkinson, Pergamon, Oxford, 1987, vol. 5, p. 861.
2 R. J. Puddephatt, *The Chemistry of Gold*, Elsevier, Amsterdam, 1978.
3 C. A. McAuliffe and W. Levason, *Phosphine, Arsine and Stibine Complexes of the Transition Elements*, Elsevier, Amsterdam, 1979.
4 S. Ahrland, K. Dreisch, B. Norén and Å. Oskarsson, *Acta Chem. Scand., Ser. A*, 1987, **41**, 173.
5 K. Angermaier, E. Zeller and H. Schmidbaur, *J. Organomet. Chem.*, 1994, **472**, 371.
6 H. Schmidbaur, G. Weidenhiller, O. Steigelmann and G. Müller, *Chem. Ber.*, 1990, **123**, 285.
7 D. B. Dyson, R. V. Parish, C. A. McAuliffe, D. G. Pritchard, R. Fields and B. Beagley, *J. Chem. Soc., Dalton Trans.*, 1989, 907.
8 P. A. Bates and J. M. Waters, *Inorg. Chim. Acta*, 1985, **98**, 125.
9 S. Ahrland, B. Aurivillius, K. Dreisch, B. Norén and Å. Oskarsson, *Acta Chem. Scand.*, 1992, **46**, 262.
10 H. Schmidbaur, G. Weidenhiller, O. Steigelmann and G. Müller, *Z. Naturforsch., Teil B*, 1990, **45**, 747.
11 H. Schmidbaur, P. Bissinger, J. Lachmann and O. Steigelmann, *Z. Naturforsch., Teil B*, 1992, **47**, 1711.
12 H. Schmidbaur, W. Graf and G. Müller, *Angew. Chem.*, 1988, **100**, 439; *Angew. Chem., Int. Ed. Engl.*, 1988, **27**, 417.
13 H. Schmidbaur, K. Dziwok, A. Grohmann and G. Müller, *Chem. Ber.*, 1989, **122**, 893.
14 K. Dziwok, J. Lachmann, D. L. Wilkinson, G. Müller and H. Schmidbaur, *Chem. Ber.*, 1990, **123**, 423.
15 A. Stützer, P. Bissinger and H. Schmidbaur, *Chem. Ber.*, 1992, **125**, 367.
16 H. Schmidbaur, A. Stützer and P. Bissinger, *Z. Naturforsch., Teil B*, 1992, **47**, 640.
17 P. Pyykkö and Y. Zhao, *Angew. Chem.*, 1991, **103**, 622; *Angew. Chem., Int. Ed. Engl.*, 1991, **30**, 604.
18 J. Li and P. Pyykkö, *Chem. Phys. Lett.*, 1992, **197**, 586.
19 P. Pyykkö, J. Li and N. Runeberg, *Chem. Phys. Lett.*, 1994, **218**, 133.
20 D. Perreault, M. Drouin, A. Michel, V. M. Miskowski, W. P. Schaefer and P. D. Harvey, *Inorg. Chem.*, 1992, **31**, 695.
21 D. A. Duddell, P. L. Goggin, R. J. Goodfellow, M. G. Norton and J. G. Smith, *J. Chem. Soc. A*, 1970, 545.
22 E. M. Menger and W. S. Veeman, *J. Magn. Reson.*, 1982, **46**, 257.
23 A. C. Olivieri, *J. Magn. Res.*, 1989, **81**, 201.
24 A. Olivieri, *J. Am. Chem. Soc.*, 1992, **114**, 5758.
25 R. K. Harris and A. C. Olivieri, *Prog. Nucl. Magn. Reson. Spectrosc.*, 1992, **24**, 435.
26 A. C. Olivieri, *J. Magn. Reson., Ser. A*, 1993, **101**, 313.
27 A. C. Olivieri, *Solid State Nucl. Magn. Reson.*, 1993, **1**, 345.
28 L.-J. Baker, G. A. Bowmaker, P. C. Healy, B. W. Skelton and A. H. White, *J. Chem. Soc., Dalton Trans.*, 1992, 989.
29 P. F. Barron, L. M. Engelhardt, P. C. Healy, J. Oddy and A. H. White, *Aust. J. Chem.*, 1987, **40**, 1545.
30 L.-J. Baker, R. C. Bott, G. A. Bowmaker, P. C. Healy, B. W. Skelton, P. Schwerdtfeger and A. H. White, *J. Chem. Soc., Dalton Trans.*, 1995, 1341.
31 M. L. Luetkens, jun., A. P. Sattelberger, H. H. Murray, J. D. Basil and J. P. Fackler, jun., *Inorg. Synth.*, 1990, **28**, 305.
32 P. L. Goggin, R. J. Goodfellow, S. R. Haddock, F. J. S. Reed, J. G. Smith and K. M. Thomas, *J. Chem. Soc., Dalton Trans.*, 1972, 1904; K. C. Dash and H. Schmidbaur, *Chem. Ber.*, 1973, **106**, 1221; F. Bonati and G. Minghetti, *Gazz. Chim. Ital.*, 1973, **103**, 373.
33 F. G. Mann, A. F. Wells and D. Purdie, *J. Chem. Soc.*, 1937, 1828.
34 P. Braunstein and R. J. H. Clark, *J. Chem. Soc., Dalton Trans.*, 1973, 1845.
35 G. M. Sheldrick, SHELXTL PLUS, Release 4.0, Siemens Analytical X-Ray Instruments, Madison, WI, 1989.
36 A. Håkansson and L. Johansson, *Chem. Scr*, 1975, **7**, 201.
37 G. A. Bowmaker and S. F. Hannan, *Aust. J. Chem.*, 1971, **24**, 2237.
38 S. Ahrland, B. Aurivillius, K. Dreisch, B. Noren and A. Oskarsson, *Acta Chem. Scand.*, 1992, **46**, 262.
39 H. G. M. Edwards and D. W. Farwell, *J. Mol. Struct.*, 1989, **197**, 203.
40 C. F. Shaw and R. S. Tobias, *Inorg. Chem.*, 1973, **12**, 965.
41 A. G. Jones and D. B. Powell, *Spectrochim. Acta, Part A*, 1974, **30**, 563.
42 G. A. Bowmaker, Effendy, J. V. Hanna, P. C. Healy, B. W. Skelton and A. H. White, *J. Chem. Soc., Dalton Trans.*, 1993, 1387.
43 G. A. Bowmaker and D. A. Rogers, *J. Chem. Soc., Dalton Trans.*, 1984, 1249.
44 M. M. El-Etri and W. M. Scovell, *Inorg. Chem.*, 1990, **29**, 480.
45 G. A. Bowmaker, *Adv. Spectrosc.*, 1987, **14**, 1.
46 K. Shobatake and K. Nakamoto, *J. Am. Chem. Soc.*, 1970, **92**, 3332.
47 N. Mohan, A. Müller and K. Nakamoto, *Adv. Infrared Raman Spectrosc.*, 1975, **1**, 173.
48 G. A. Bowmaker, R. D. Hart, B. E. Jones, B. W. Skelton and A. H. White, *J. Chem. Soc., Dalton Trans.*, 1995, 3063.
49 G. A. Bowmaker and R. Whiting, *Aust. J. Chem.*, 1976, **29**, 1407.
50 G. A. Bowmaker and P. C. Healy, *Spectrochim. Acta, Part A*, 1988, **44**, 115.
51 G. A. Bowmaker, P. C. Healy, J. D. Kildea and A. H. White, *Spectrochim. Acta, Part A*, 1988, **44**, 1219.
52 G. Bouquet and M. Bigorgne, *Spectrochim. Acta, Part A*, 1967, **23**, 1231.
53 G. A. Bowmaker, J. D. Cotton, P. C. Healy, J. D. Kildea, S. B. Silong, B. W. Skelton and A. H. White, *Inorg. Chem.*, 1989, **28**, 1462.
54 S. J. Berners-Price, L. A. Colquhoun, P. C. Healy, K. A. Byriel and J. V. Hanna, *J. Chem. Soc., Dalton Trans.*, 1992, 3357.
55 P. G. Jones, A. G. Maddock, M. J. Mays, M. M. Muir and A. F. Williams, *J. Chem. Soc., Dalton Trans.*, 1977, 1434.
56 J. G. Verkade and J. A. Mosbo, in *Phosphorus-31 N.M.R. Spectroscopy in Stereochemical Analysis*, eds. J. G. Verkade and L. D. Quin, VCH, Deerfield Beach, FL, 1987, pp. 425–463.

Received 5th February 1996; *Paper* 6/00823B